Applied Catalysis A: General 505 (2015) 36–43

Contents lists available at ScienceDirect

Applied Catalysis A: General

journal homepage: www.elsevier.com/locate/apcata

Glycerol etherification with benzyl alcohol over sulfated zirconia catalysts

María A. Jaworski[a,b], Sergio Rodríguez Vega[c], Guillermo J. Siri[a,b], Mónica L. Casella[a,*], Arturo Romero Salvador[c], Aurora Santos López[c]

[a] CINDECA, CCT La Plata-CONICET, Departamento de Química, Facultad de Ciencias Exactas, Universidad Nacional de La Plata, calle 47 No 257, 1900 La Plata, Argentina
[b] PIDCAT, Facultad de Ingeniería, Universidad Nacional de La Plata, calle 1 y 47, 1900 La Plata, Argentina
[c] Departamento de Ingeniería Química, Facultad de Ciencias Químicas, Universidad Complutense de Madrid, Ciudad Universitaria, 28040 Madrid, Spain

ARTICLE INFO

Article history:
Received 29 December 2014
Received in revised form 14 April 2015
Accepted 18 April 2015
Available online 2 May 2015

Keywords:
Glycerol
Benzyl alcohol
Etherification
Sulfated zirconia catalysts
Kinetic modeling

ABSTRACT

Glycerol (GLY) etherification with benzyl alcohol (BA) was conducted with different zirconia-based heterogeneous acid catalysts, aiming to produce mono- (ME) and dibenzyl glycerol ethers (DE). Physicochemical properties of the prepared catalysts were obtained through XRD, SEM and adsorption of ammonia. The catalytic tests were performed at different temperatures (120–140 °C) and initial reactant mass ratios (GLY:BA 1:1 and 2:1). The highest BA conversions were obtained with the catalyst having the highest sulfuric acid content ($2S/ZrO_2$). An increase in the reaction temperature and the GLY:BA initial mass ratio led to an increase in the BA conversion. Two kinetic models (a potential and a hyperbolic approach) were proposed to describe the process performance, including not only reactants evolution with time, but also that of ME, DE and the undesired self-condensation product of BA (benzyl ether, BE). Kinetic parameters for each model were estimated by data fitting and both models were able to accurately describe the evolution of the system, in terms of reactants and product distribution as a function of time under the experimental conditions studied.

1. Introduction

Biodiesel (monoalkyl esters of long chain fatty acids) is an alternative diesel fuel derived from the reaction of vegetable oils or lipids and a short chain alcohol [1]. The new energy legislation implemented in Europe promotes the use of biofuels for transport purposes. Thus, traffic fuels should contain 10% of energy content produced from renewable sources by the end of 2020 [2]. In this context, the production of biodiesel in the European Union is expected to grow further in the next years [3]. The catalytic process that converts raw triglycerides into biodiesel also produces important quantities of glycerol as side product: for every ton of biodiesel produced, around 100 kg of glycerol is formed [4].

Due to the growing biodiesel production, the price of glycerol significantly dropped, making it one of the most promising platform chemicals of the near future. Moreover, using glycerol as starting raw material for the synthesis of value-added chemicals is of great industrial importance, because it is also a nontoxic, edible, sustainable and biodegradable compound [5].

A large portfolio of reaction pathways for catalytic conversion of glycerol is available, including selective oxidation, selective hydrogenolysis to propanediol, dehydration to acrolein, pyrolysis and gasification, steam reforming, thermal reduction to syngas, oligomerization/polymerization, selective transesterification, etherification to fuel-oxygenates, conversion into glycerol carbonate and synthesis of epichlorohydrin [5,6].

Concerning the etherification reaction, the selective mono- or di-etherification of glycerol with alcohols using acid catalysts originates chemicals with high-added value [3,7]. Glycerol ethers have been identified as valuable replacement of fuel additives, which depends on depleting sources, price uncertainty and growing environmental concern of petroleum feedstock. These glycerol-based fuel additives are excellent additives with large potential for diesel and biodiesel formulation that assist to a decreasing in particles, hydrocarbons, carbon monoxide and unregulated aldehydes emissions [1,5]. Besides, these glycerol-based additives seem to catch the motivation and interest of many researchers lately because

Abbreviations: BA, benzyl alcohol; BE, benzyl ether; DE, di-benzyl glycerol ether; GLY, glycerol; ME, mono-benzyl glycerol ether; TE, tri-benzyl glycerol ether; W, water.

* Corresponding author. Tel.: +54 2214210711.
E-mail address: casella@quimica.unlp.edu.ar (M.L. Casella).

http://dx.doi.org/10.1016/j.apcata.2015.04.027
0926-860X/

Nomenclature

C_{io}	concentration at zero time of specie *i* (mol/kg)
C_i	concentration at time *t* of specie *i* (mol/kg)
E_{aj}	activation energy of reaction *j* (kJ/mol)
$I_m(\bar{1}\ 1\ 1)$	line intensities of the $(\bar{1}\ 1\ 1)$ (at $2\theta = 28.2°$) peaks for the monoclinic phase (m-ZrO_2)
$I_m(1\,1\,1)$	line intensities of the (1 1 1) (at $2\theta = 31.5°$) peaks for the monoclinic phase (m-ZrO_2)
k_j	kinetic constant of reaction *j* (kg/mol min)
k_{0j}	pre-exponential factor of kinetic constant k_j in reaction *j* (kg/mol min)
K_{GLY}	equilibrium constant of glycerol adsorption (kg/mol)
r_j	rate of reaction *j* (mol/kg min)
R_i	production rate of specie *i* in the batch reactor (mol/kg min)
S	selectivity of the 2S/ZrO_2 catalyst, defined in Eq. (X).
S_g	*BET* specific surface area ($m^2\,g^{-1}$)
T	reaction temperature (°C)
t	reaction time (min)
V_p	pore volume ($cm^3\,g^{-1}$)
X_{BA}	benzyl alcohol conversion defined according to Eq. (2)
X_m	fraction of the monoclinic phase of zirconia according to Eq. (1)
Y	global yield of the 2S/ZrO_2 catalyst, defined in Eqs. (3)–(5)

this approach is a promising and economically viable alternative since not only makes a good use of the glycerin by-product but also increases the yield to biofuel in the overall biodiesel production process [3,8].

Depending on the alcohol used, the selective glycerol monoetherification also leads to the production of high value added chemicals, which have a wide range of biological applications such as anti-inflammatory, antibacterial, antifungal, antitumor, among others. Thus, there have been reported in the literature some examples of the glycerol etherification with benzyl, propargyl and allyl alcohols which have resulted in the formation of the corresponding ethers in moderate yields [9].

In order to improve the yield of the etherification of glycerol different acid catalysts have been used. Da Silva et al. reported the etherification of glycerol with benzyl alcohol catalyzed by different solid acid catalysts. They found that with zeolite β and Amberlyst-35 the mono-benzyl-glycerol ether was the main product formed, whereas over K-10 montmorillonite and *p*-toluene sulfonic acid the di-benzyl ether was formed. Another solid acid catalyst, niobic acid, was inactive toward the reaction [7]. Other authors found that the best catalytic results were achieved with strong acid ion exchange resins (Amberlyst type) as catalysts, despite the temperature limitations of this kind of materials [10,11].

González et al. studied the glycerol etherification with isobutene over several types of silicas (MCM-41, SBA-15 and HMS) modified by incorporating aluminum or by introducing phosphorus species or sulfonic groups. They found that the incorporation of aluminum increased the amount of Brønsted acid sites in their structure, leading to higher catalytic activity than pure silicas, but with a low selectivity to di- and tri-tertiary butyl ethers of glycerol (h-GTBE). The introduction of phosphoric groups, with higher acidity strength, improved the selectivity to h-GTBE [12]. Also, sulfonic acid-functionalized mesostructured materials have demonstrated an excellent catalytic behavior in the transformation of glycerol into oxygenated compounds for fuel formulation [3,8,13].

In this context, the objective of this work is to study the glycerol (GLY) etherification with benzyl alcohol (BA), using zirconia-based heterogeneous acid catalysts prepared at our laboratory, aiming to produce mono- (ME) and di-benzyl glycerol ethers (DE). A non-desired reaction, the self-condensation of benzyl alcohol yielding benzyl ether (BE), can be also produced (as showed in Scheme 1). Experiments were conducted varying the operative conditions (temperature and GLY:BA concentration ratio) and two kinetic models were proposed to explain the results obtained.

2. Experimental

2.1. Catalyst preparation

For the preparation of ZrO_2, a procedure described elsewhere was followed [14]. The precursor salt, $ZrOCl_2{\cdot}8H_2O$ (*Fluka*), was dissolved in distilled water and aqueous ammonia was added until the pH of the solution reached a value of 10 and the formation of the gel was observed. The mixture was aged for 8 days at room temperature. The obtained precipitate was washed with distilled water until free from chloride ions (determined by $AgNO_3$), filtered and dried at 105 °C for 24 h. The hydrous zirconia was calcined at 600 °C for 2 h. The following equation represents the zirconia preparation:

$$ZrOCl_2 \cdot 6H_2O + OH^- \rightarrow ZrO_2 + 2Cl^- + H^+ + 6H_2O$$

To prepare sulfated zirconia, a portion of hydrous zirconia was mixed with an appropriate volume of either 1 M or 2 M H_2SO_4 (*Merck p.a.*) and stirred for 24 h. After filtration, the sample was dried at 105 °C and calcined for 2 h at 600 °C to form 1S/ZrO_2 and 2S/ZrO_2, respectively.

2.2. Catalyst characterization

The textural properties of the solids (specific surface area, S_{BET}, and pore volume) were measured by N_2 adsorption–desorption at −196 °C using a *Micromeritics Accusorb 2100E* apparatus. The S_{BET} was calculated by the BET equation and the pore volume (V_p) was estimated using the adsorption branch of the nitrogen isotherm curve at $P/P_0 = 0.98$ single point. The textural properties of the catalysts are listed in Table 1.

The structural characterization was completed by X-ray powder diffraction (XRD) performed on a *Philips PW 1050/70* diffractometer using Cu Kα radiation (λ = 0.154 nm). XRD data were recorded in the range of $2\theta = 5$–70° at a scanning speed of 2° min^{-1}. The fractions of the monoclinic and tetragonal phases of zirconia were calculated with the following equation [15]:

$$X_m = \frac{I_m\left(\bar{1}\ 1\ 1\right) + I_m(1\ 1\ 1)}{I_m\left(\bar{1}\ 1\ 1\right) + I_m(1\ 1\ 1) + I_t(1\ 0\ 1)} \quad (1)$$

where $I_m(\bar{1}\ 1\ 1)$ and $I_m(1\,1\,1)$ are the line intensities of the $(\bar{1}\ 1\ 1)$ (at $2\theta = 28.2°$) and (1 1 1) (at $2\theta = 31.5°$) peaks for the monoclinic phase (m-ZrO_2) and $I_t(1\,0\,1)$ is the intensity of the (1 0 1) (at $2\theta = 30.2°$) peak for the tetragonal phase (*t*-ZrO_2) of zirconium oxide.

The total acidity of the prepared catalysts was studied by adsorption of ammonia using a thermobalance (*Shimadzu TGA 50*). In a typical procedure, the sample was dried in a He flow (30 mL min^{-1}) by heating from room temperature up to 500 °C at a rate of 10 °C min^{-1} to remove adsorbed water and other volatiles. Then, the sample was cooled in a He flow to 70 °C. At that temperature, the catalyst was exposed to an NH_3–He mixture (5 vol%) at 60 mL min^{-1} flow for the adsorption of the base, until a constant weight was obtained.

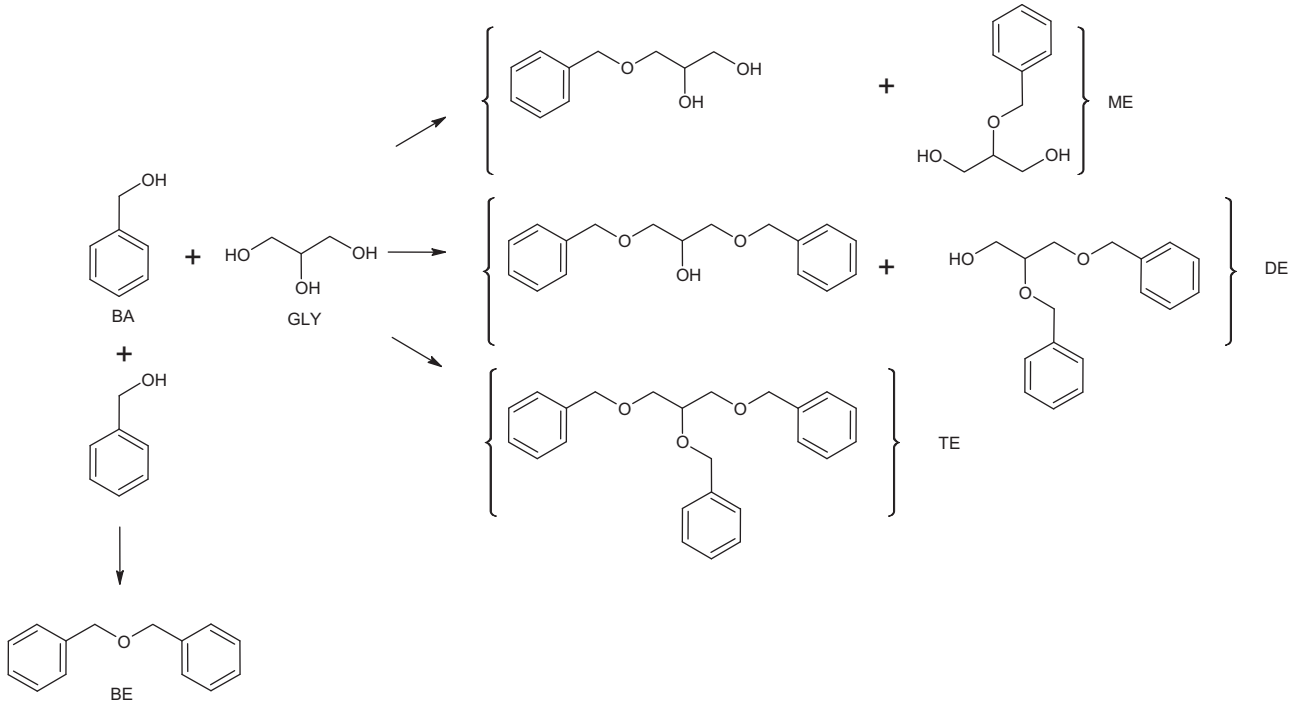

Scheme 1. Reaction pathway proposed for the catalytic etherification of glycerol (GLY) with benzyl alcohol (BA). Reaction products: glyceryl monobenzyl ethers (ME); glyceryl dibenzyl ethers (DE); glyceryl tribenzyl ether (TE) and benzyl ether (BE) (a non-desired product, form through the self-condensation of BA).

SEM/EDX measurements were carried out using a *FEI Quanta 200* scanning electron microscope equipped with an energy dispersive X-ray spectroscopy facility (EDX SDD Apollo 40).

2.3. Catalytic test

The glycerol (GLY) etherification with benzyl alcohol (BA) was performed in a glass reactor vessel (50 mL) at atmospheric pressure, under continuous stirring and with a temperature controller. The reaction was conducted at different temperatures ranged between 120 °C and 140 °C for 6 h under continuous N_2 gas flow to avoid glycerol oxidation and to remove water formed from the reaction. GLY:BA initial mass ratios used were 1:1 and 2:1 and catalyst concentration was 25 g/kg, referred to the total initial mass of reactants. The stirring speed was selected in order to limit external mass transfer effects. In a typical run, once the reaction temperature had been reached, the appropriate amounts of anhydrous GLY and catalyst were added into the reactor and this time has been considered as the starting point of the reaction. The liquid samples obtained from the etherification of GLY were collected at specific intervals during the reaction and the reaction products were analyzed by GC/MS in an Agilent 6890 chromatograph (*Agilent Technologies*, USA). The chromatograph was equipped with an HP Innowax chromatographic column with the following dimensions: 60 m length × 0.32 mm i.d. and 0.25 μm film thickness. Initial oven temperature was 90 °C and final oven temperature was 250 °C, with two programmed temperature ramps of 1 and 3 °C min^{-1}.

3. Results and discussion

3.1. Catalyst characterization

The physicochemical properties of ZrO_2, 1S/ZrO_2 and 2S/ZrO_2 catalysts were examined by X-ray powder diffraction, BET surface area and TG analysis of ammonia adsorption. The XRD patterns of the three catalysts are shown in Fig. 1. The corresponding phase composition, BET surface area, pore volume and acidity results are presented in Table 1. As can be seen from Fig. 1, the ZrO_2 sample calcined at 600 °C presents a mixture of monoclinic and tetragonal phases, with a prevalence of the monoclinic one (see also Table 1). On the other hand, the sulfated samples exhibit prominent lines due to tetragonal phase, indicating that the impregnated sulfate ions show a strong influence on the phase modification of zirconia from thermodynamically more stable monoclinic to the metastable tetragonal phase [16,17].

ZrO_2 sample has a specific surface area of 45 m^2 g^{-1}, presenting a weak acidity (see Table 1). The inclusion of sulfate anions in 1S/ZrO_2 and 2S/ZrO_2 not only favors an increment of the surface area but of the acidity of the catalysts as well, clearly indicating that impregnated sulfate ions show a strong influence on the acidic properties of the zirconia. Total pore volume slightly increases with the incorporation of sulfuric acid. From results in Fig. 2 showing the SEM micrographs of the ZrO_2, 1S/ZrO_2 and 2S/ZrO_2 catalysts, it is noticed that irregular edge-shaped large particles are obtained for the three catalysts. At the microscopic scale, the surface of the samples appears to be porous, as can be seen in Fig. 2. No significant

Table 1
Physicochemical characteristics of the studied catalysts.

Catalyst	S_g BET (m^2 g^{-1})	Pore volume (cm^3 g^{-1})	Crystalline phase of ZrO_2[a]	Acidity[b] (mmol NH_3 ads $gcat^{-1}$)
ZrO_2	45	0.11	M (90%) and T	0.068
1S/ZrO_2	89	0.08	T	0.125
2S/ZrO_2	92	0.09	T	0.248

[a] M, monoclinic phase; T, tetragonal phase.
[b] Measured by TGA.

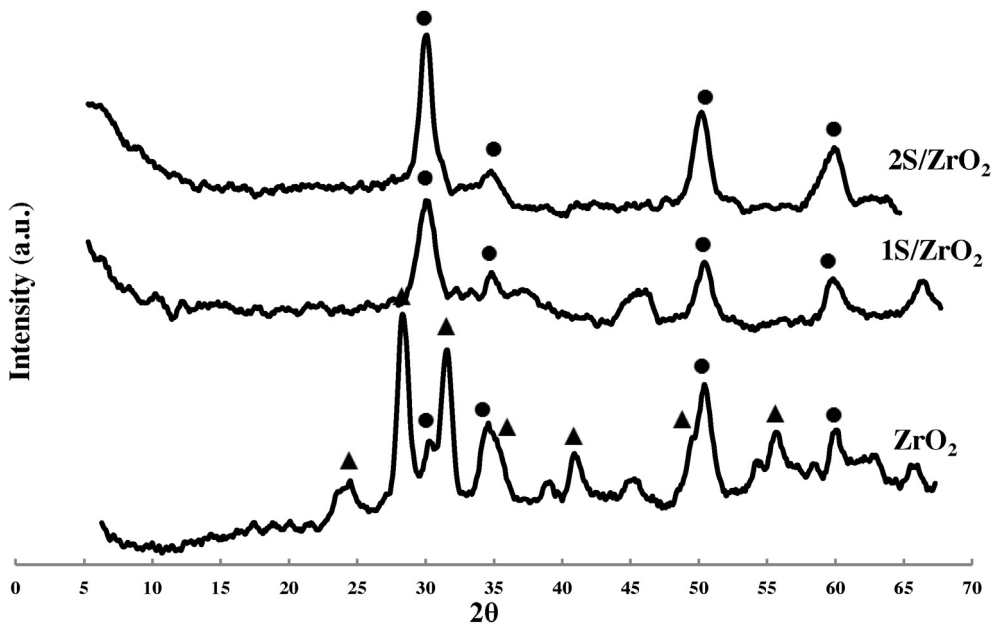

Fig. 1. XRD patterns of calcined zirconia (ZrO_2) and sulfated zirconia ($1S/ZrO_2$ and $2S/ZrO_2$) catalysts. (▲) Characteristic lines due to monoclinic zirconia; (●) characteristic lines due to tetragonal zirconia.

change in the morphology has been noted after impregnation of sulfate.

3.2. Catalytic results

All the prepared catalysts were evaluated in the GLY etherification using BA as active alcohol, at a reaction temperature of 120 °C. The results indicated that ZrO_2 was inactive for this reaction in the operating condition range used, while both sulfated zirconia-based catalysts were active. This behavior can be explained taking into account the well-known fact that the etherification of alcohols is a reaction catalyzed by acids. In the presence of an acidic catalyst, a hydroxyl group of an alcohol is protonated, which renders it a good leaving group. Considering the pKa values of GLY (14.15) and BA (15.40), the lower acidity of BA favors its protonation versus GLY. Accordingly, the protonation of BA is produced by action of the acid catalyst, and when it loses a water molecule a carbocation is formed, which is in turn attacked by a OH^-, either of GLY or of another BA molecule. This allows to explain the formation of BE, and also the fact that there have not been observed neither aldehydes nor GLY dimers.

Based on these results, the influence of some experimental variables was evaluated for both sulfated zirconia catalysts, $1S/ZrO_2$ and $2S/ZrO_2$.

3.2.1. Influence of acidity

The effect of the content of sulfuric acid in the preparation of the sulfated zirconia catalysts was analyzed in the etherification of GLY with BA in equal initial mass ratio. Fig. 3a compares the evolution of the conversion of BA as a function of time (t) at 120 °C for both $1S/ZrO_2$ and $2S/ZrO_2$ catalysts, while Fig. 3b shows the same progress when the reaction was carried out at 140 °C.

BA conversion was defined according to Eq. (2), being C_{BAo} and C_{BA} the benzyl alcohol concentration at zero and t times, respectively (mol/kg).

$$X_{BA} = \frac{C_{BAo} - C_{BA}}{C_{BAo}} \quad (2)$$

Fig. 3 The results presented in Fig. 3a and b clearly show that a higher BA conversion is obtained using the catalyst with the higher sulfuric acid content and that this difference in activity is most noticeable when the temperature is increased from 120 °C to 140 °C. The greater activity of $2S/ZrO_2$ catalyst at the same temperature can be associated with its higher acidity presented in Table 1. This same trend has been found by Pico et al. who studied the glycerol etherification with *tert*-butyl alcohol using cationic exchange resins with different acidity [18].

3.2.2. Influence of temperature

The effect of temperature on the catalytic activity of the system that showed the best performance, $2S/ZrO_2$, was evaluated with

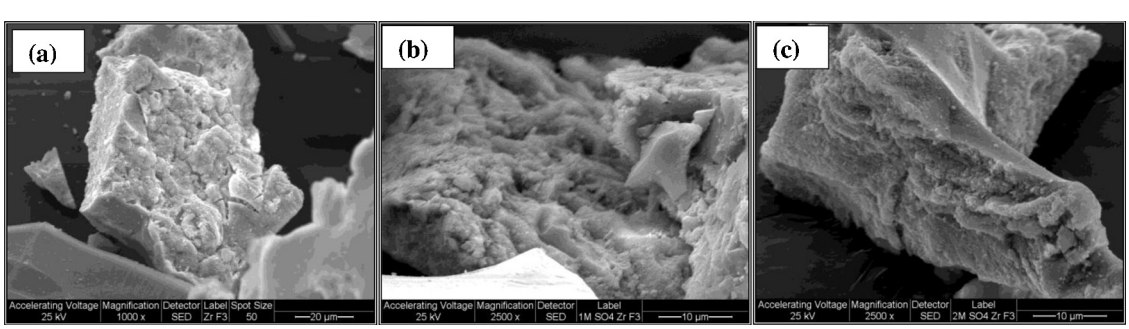

Fig. 2. SEM micrographs of the studied samples: (a) ZrO_2; (b) $1S/ZrO_2$ and (c) $2S/ZrO_2$.

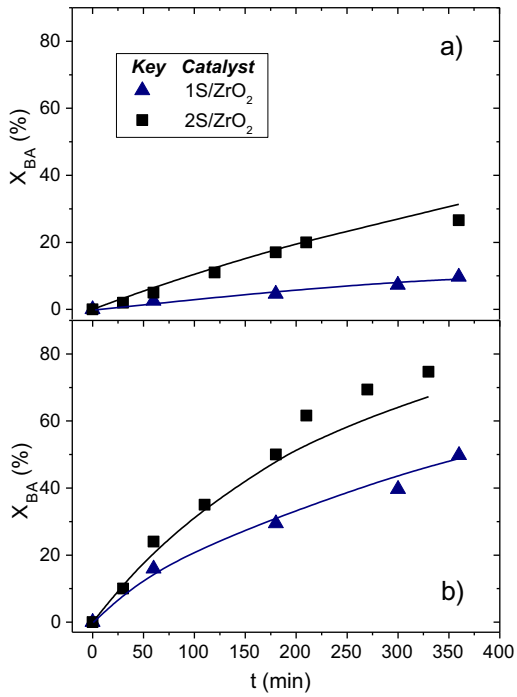

Fig. 3. Evolution of BA conversion with time employing 1S/ZrO_2 and 2S/ZrO_2 catalysts. GLY:BA initial mass ratio 1:1. Catalyst concentration: 25 g/kg. Reaction temperature: (a) 120 °C and (b) 140 °C.

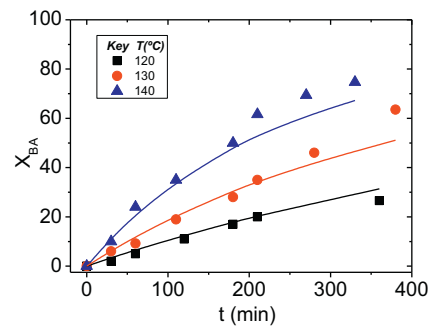

Fig. 4. Evolution of BA conversion with time employing 2S/ZrO_2 catalysts. Catalyst concentration: 25 g/kg; initial GLY:BA mass ratio 1:1. Reaction temperature: 120 °C, 130 °C and 140 °C. Symbols: experimental data. Lines: estimated with potential kinetic model.

some more detail. To do this, BA conversion obtained at temperatures of 120, 130 and 140 °C were plotted in Fig. 4. As expected, the trend toward greater activity with increased temperature was confirmed. The upper temperature limit was set taking into account the vapor pressure of BA.

Global Yield (Y) and Selectivity (S) of the 2S/ZrO_2 catalyst to sum of monoethers (Y_{ME}, S_{ME}), sum of diethers (Y_{DE}, S_{DE}) and benzyl ether (Y_{BE}, S_{BE}) has been defined as:

$$Y_{ME}(\%) = \frac{C_{ME}}{C_{BAo}} \cdot 100 \quad S_{ME}(\%) = \frac{C_{ME}}{C_{ME} + C_{DE} + 2C_{BE}} \cdot 100 \tag{3}$$

$$Y_{DE}(\%) = \frac{C_{DE}}{C_{BAo}} \cdot 100 \quad S_{DE}(\%) = \frac{C_{DE}}{C_{ME} + C_{DE} + 2C_{BE}} \cdot 100 \tag{4}$$

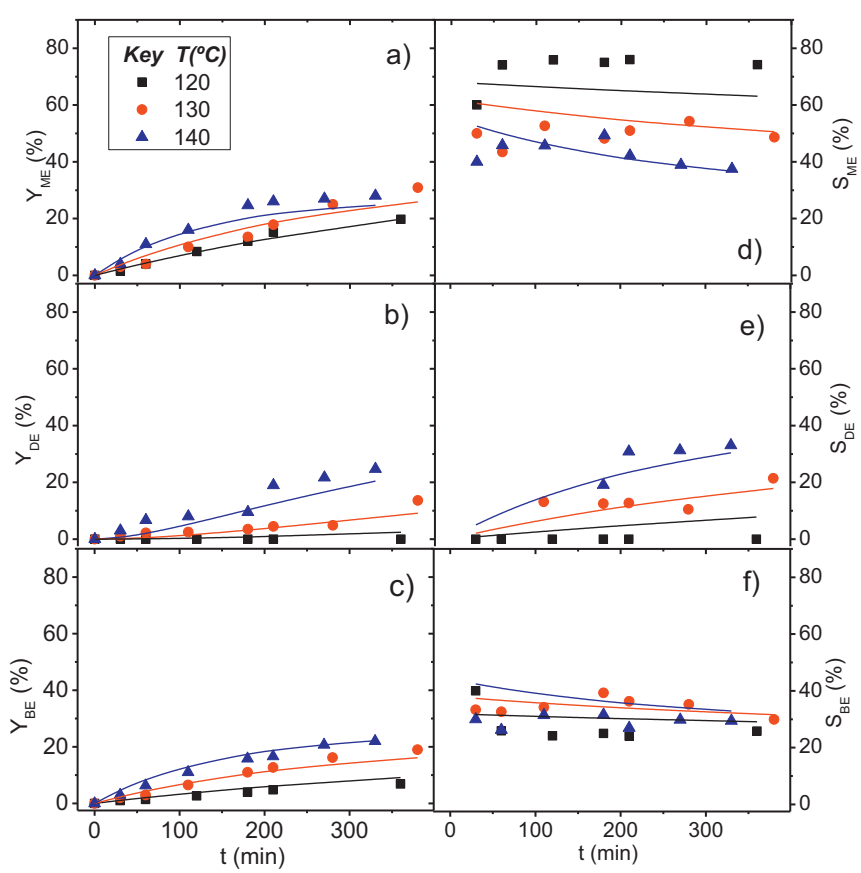

Fig. 5. Global yield of ME (a), DE (b) and BE (c) and selectivity to ME (d), DE (e) and BE (f). Catalyst concentration: 25 g/kg; initial GLY:BA mass ratio 1:1. Reaction Temperature: 120 °C, 130 °C and 140 °C. Symbols: experimental data. Lines: estimated with potential kinetic model.

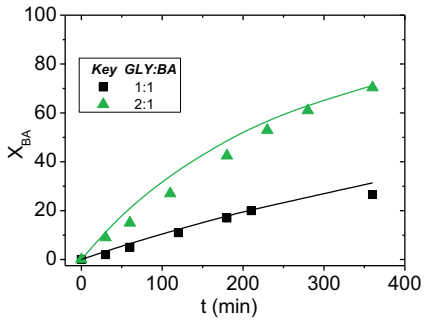

Fig. 6. Influence of the reactants ratio on the evolution of BA conversion with time. GLY:BA initial mass ratio of 1:1 and 2:1. Catalyst: 2S/ZrO_2 (25 g/kg). Reaction temperature: 120 °C. Symbols: experimental data. Lines: estimated with potential kinetic model.

$$Y_{BE}(\%) = \frac{C_{BE}}{C_{BAo}} \cdot 100 \quad S_{BE}(\%) = \frac{C_{BE}}{C_{ME} + C_{DE} + 2C_{BE}} \cdot 100 \tag{5}$$

Being C_{ME}, C_{DE} and C_{BE} the monoethers, diethers and benzyl ether concentration, respectively, expressed as mol/kg. Obviously, from Eqs (2)–(5) it is deduced that:

$$X_{BA} = Y_{ME} + Y_{DE} + Y_{BE} \tag{6}$$

Global yield and selectivity obtained at reaction temperatures of 120–140 °C with a GLY to BA mass ratio of 1:1 are shown in Fig. 5. As shown in this figure, the selectivity to ME decreases with time and with temperature, as a result of the formation of DE through a consecutive reaction. In turn, a slight decrease in the BE selectivity with reaction time is noticed. Temperature has a lower effect in selectivity to BE.

3.2.3. *Influence of reactants ratio*

The effect of the initial concentration of the reactants was studied at 120 °C, using two GLY:BA initial mass ratios, 1:1 and 2:1. The results of BA conversion versus time are plotted in Fig. 6. As can be seen, a higher concentration of GLY causes an increase in BA conversion.

The global yield and selectivity of ME, DE and BE at the two GLY to BA initial mass ratios tested (1:1 and 2:1) at 120 °C can be seen in Fig. 7. As can be seen in this figure, the yield and selectivity to desired products (ME and DE) increased with higher amounts of GLY. While the yield to BE was slightly increased (because BA conversion also did), the selectivity to this undesirable product decreased when initial GLY:BA was increased.

3.3. *Kinetic modeling*

Two kinetic strategies, summarized in Table 2 were proposed to describe glycerol etherification with benzyl alcohol: a potential and a hyperbolic kinetic model, where only GLY is considered to be adsorbed in the catalyst surface. Both models were developed

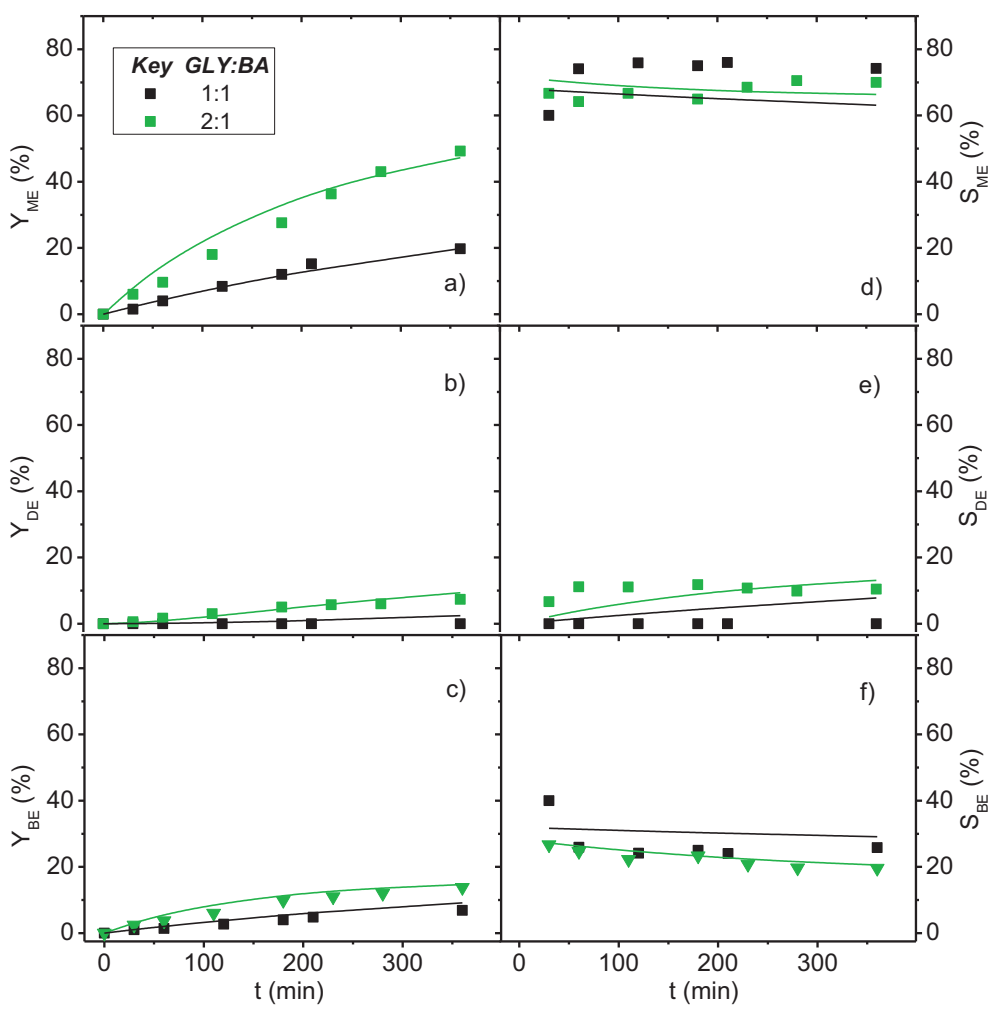

Fig. 7. Influence of the reactants ratio on the global yield of ME (a), DE (b) and BE (c) and on the selectivity to ME (d), DE (e) and BE (f). GLY:BA initial mass ratio of 1:1 and 2:1. Catalyst: 2S/ZrO_2 (25 g/kg). Reaction Temperature: 120 °C. Symbols: experimental data. Lines: estimated with potential kinetic model.

Table 2
Potential kinetic model and hyperbolic kinetic model for the catalytic etherification of glycerol with benzyl alcohol.

Reaction	Stoichiometric equation	Reaction rate	
		Potential model	Hyperbolic model
1	$Gly + BA \rightarrow ME + W$	$r_1 = k_1 C_{BA} C_{Gly}$	$r_1 = \frac{k_1 C_{BA} C_{GLY}}{1 + K_{GLY} C_{GLY}}$
2	$BA + ME \rightarrow DE + W$	$r_2 = k_2 C_{BA} C_{ME}$	$ar_2 = \frac{k_2 C_{BA} C_{ME}}{1 + K_{GLY} C_{GLY}}$
3	$2BA \rightarrow BE + W$	$r_3 = k_3 C_{BA}^2$	$r_3 = \frac{k_3 C_{BA}^2}{1 + K_{GLY} C_{GLY}}$

Table 3
Mass balance of reactants and products in a batch reactor involved in the catalytic GLY etherification with BA. BA, BE and ME selected as key compounds.

Compound	Concentration
Benzyl alcohol (BA)	$C_{BA} = C_{BA_0} - \int_0^t (r_1 + r_2 + 2r_3)dt$
Dibenzyl ether (BE)	$C_{BE} = \int_0^t (r_3)dt$
Monobenzyl glycerol ether (ME)	$C_{ME} = \int_0^t (r_1 - r_2)dt$
Glycerol (GLY)	$C_{Gly} = C_{Gly0} - C_{ME} - C_{DE} = C_{Gly0} - \frac{C_{ME}}{2} - \frac{C_{BA0} - C_{BA}}{2} + C_{BE}$
Dibenzyl glycerol ether (DE)	$C_{DE} = \frac{C_{BA0} - C_{BA} - 2C_{BE} - C_{ME}}{2}$

Table 4
Kinetic and statistical parameters obtained for the catalytic GLY etherification with BA using the potential kinetic model.

Parameter	Value	Standard error
$\frac{E_{a1}}{R}(K)$	8.5×10^3	5.36×10^2
$\frac{E_{a2}}{R}(K)$	1.33×10^4	3.29×10^3
$\frac{E_{a3}}{R}(K)$	1.29×10^4	1.21×10^2
$\ln k_{1o}$	12.8	1.31
$\ln k_{2o}$	25.9	8.01
$\ln k_{3o}$	22.7	2.96

Table 5
Kinetic and statistical parameters obtained for the catalytic GLY etherification with BA using the hyperbolic kinetic model.

Parameter	Value	Standard error
$\frac{E_{a1}}{R}(K)$	1.26×10^4	9.59×10^2
$\frac{E_{a2}}{R}(K)$	8.80×10^3	3.86×10^2
$\frac{E_{a3}}{R}(K)$	1.21×10^4	2.46×10^3
$\ln k_{1o}$	24.3	23.4
$\ln k_{2o}$	14.8	9.42×10^{-1}
$\ln k_{3o}$	24.1	5.97

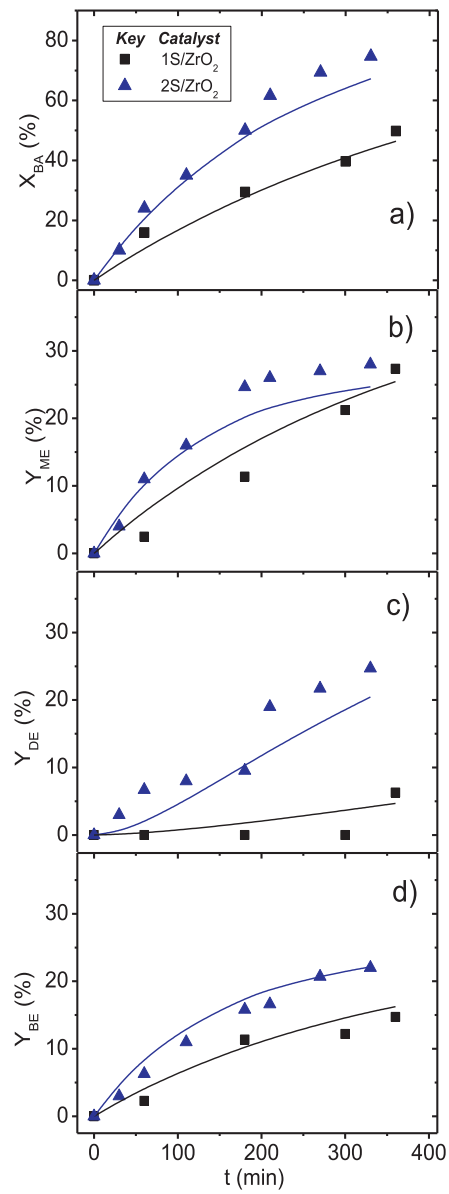

Fig. 8. Evolution of (a) BA conversion with time and global yield of (b) ME, (c) DE and (d) BE. GLY to BA mass ratio of 1:1. Catalyst $1S/ZrO_2$ and $2S/ZrO_2$ (25 g/kg). Reaction Temperature 140 °C. Symbols: experimental data. Lines: estimated with potential kinetic model.

according to the reaction pathway shown in Scheme 1. The water content was considered to be negligible because of reaction conditions, which approaches the system to irreversible. Reaction rates for both models can be seen in Table 2, where the effect of reaction temperature is included in the kinetic constants considered as temperature-dependent according to the Arrhenius equation:

$$k_j = k_o \exp\left(\frac{-E_{aj}}{RT}\right)$$

Three key compounds were selected, BA, BE and ME. From the mass balance in a batch reactor, the evolution of the concentration of this key compounds with time can be obtained, according to equations shown in Table 3 while the concentration of GLY and DE can be obtained from this key compounds by stoichiometry (also summarized in Table 3).

Results obtained with $2S/ZrO_2$ catalyst at different temperatures (120–140 °C) and initial mass ratios of reactants (1:1 and 2:1) were used to develop both kinetic models, the potential and the

hyperbolic approach. Kinetic parameters in Tables 2 and 3 were calculated by experimental data fitting (concentrations of BA, BE and ME as a function of time). Nonlinear regression (Marquadt algorithm) was coupled with a Runge–Kutta integration step in the fitting procedure. The kinetic parameters obtained after fitting of the experimental data are summarized in Tables 4 and 5 (for potential and hyperbolic model, respectively) including their standard error values.

The sum of squares obtained with the hyperbolic model is slightly smaller than that obtained with the potential one; however both fit the experimental values in an appropriate way. In Figs. 4–7, experimental results are plotted as symbols while estimated values using the potential model are plotted as lines. As can be observed, a good agreement between experimental and predicted data is obtained, which validates the proposed kinetic models.

Fig. 8.

4. Conclusions

Two solid acid catalysts were prepared modifying the zirconia with sulfuric acid at two concentration levels: 1 and 2 M ($1S/ZrO_2$ and $2S/ZrO_2$ catalysts). The addition of sulfuric acid favored to obtain a tetragonal zirconia phase, regardless of the sulfuric content. The $2S/ZrO_2$ catalyst was the most acidic, according to the ammonia adsorption measured by TGA.

GLY etherification with BA was carried out using the prepared catalysts, both of them being active for the reaction in the range of temperatures studied. BA conversion increased with increasing temperature from 120 °C to 140 °C. The higher acidity of the catalyst, the higher activity was obtained at any temperature. The main reaction products were ME and DE, although the self-etherification of BA to give BE was also observed. By increasing the GLY:BA initial mass ratio, the BE selectivity decreased. On the contrary, as temperature increases, BE selectivity also increases. Both evidences are well explained by the kinetic model proposed and validated by data fitting.

BA self-condensation follows a second order reaction in BA with higher activation energy than the ME and DE reactions from BA, being these reactions first order in the benzyl alcohol concentration.

References

[1] J. Janau, N. Ellis, Renew. Sust. Energ. Rev. 14 (2010) 1312–1320.
[2] Directive 2009/28/EC of the European Parliament and of the Council of 23 April 2009.
[3] J.A. Melero, G. Vicente, M. Paniagua, G. Morales, P. Muñoz, Bioresour. Technol. 103 (2012) 142–151.
[4] F. Frusteri, F. Arena, G. Bonura, C. Cannilla, L. Spadaro, O. Di Blasi, Appl. Catal. A-Gen. 367 (2009) 77–83.
[5] M.V. Sivaiah, S. Robles-Manuel, S. Valange, J. Barrault, Catal. Today 198 (2012) 305–313.
[6] P.H.R. Silva, V.L.C. Gonçalves, C.J.A. Mota, Bioresour. Technol. 101 (2010) 6225–6229.
[7] C.R.B. da Silva, V.L.C. Gonçalves, E.R. Lachter, C.J.A. Mota, J. Braz. Chem. Soc. 20 (2) (2009) 201–204.
[8] J.A. Melero, G. Vicente, G. Morales, M. Paniagua, J.M. Moreno, R. Roldan, A. Ezquerro, C. Perez, Appl. Catal. A-Gen. 346 (2008) 44–51.
[9] Y. Gu, A. Azzouzi, Y. Pouilloux, F. Jérôme, J. Barrault, Green Chem. 10 (2008) 164–167.
[10] K. Klepacova, D. Mravec, A. Kaszonyi, M. Bajus, Appl. Catal. A-Gen. 328 (2007) 1–13.
[11] M.P. Pico, J.M. Rosas, S. Rodriguez, A. Santos, A. Romero, J. Chem. Technol. Biot. 88 (11) (2013) 2027–2038.
[12] M.D. González, P. Salagre, R. Mokaya, Y. Cesteros, Catal. Today 227 (2014) 171–178.
[13] M.D. González, P. Salagre, E. Taboada, J. Llorca, E. Molins, Y. Cesteros, Appl. Catal. B-Environ. 136–137 (2013) 287–293.
[14] M.A. Jaworski, I.D. Lick, G.J. Siri, M.L. Casella, Appl. Catal. B-Environ. 156–157 (2014) 53–61.
[15] H. Toraya, M. Yoshimura, S. Somiya, J. Am. Ceram. Soc. 67 (6) (1984), C-119–C-121.
[16] B.M. Reddy, P.M. Sreekanth, P. Lakshmanan, J. Mol. Catal. A-Chem. 237 (2005) 93–100.
[17] J.M. Grau, J.C. Yori, J.M. Parera, Appl. Catal. A-Gen. 213 (2001) 247–257.
[18] M.P. Pico, S. Rodríguez, A. Santos, A. Romero, Ind. Eng. Chem. Res. 52 (2013) 14545–14555.